Intel Serv Robotics (2017) 10:257–270
DOI 10.1007/s11370-017-0222-0

ORIGINAL RESEARCH PAPER

Implementing the homotopy continuation method in a hybrid approach to solve the kinematics problem of spatial parallel robots

Naser Mostashiri[1] · **Alireza Akbarzadeh**[1] · **Amir Rezaei**[1]

Received: 16 June 2016 / Accepted: 22 February 2017 / Published online: 23 March 2017
© Springer-Verlag Berlin Heidelberg 2017

Abstract In this paper, first the application of homotopy continuation method (HCM) in numerically solving kinematics problem of spatial parallel manipulators is investigated. Using the HCM the forward kinematics problem (F-Kin) of a six degrees of freedom (DOFs) 6–3 Stewart platform and the inverse kinematics problem (I-Kin) of a 3-DOF 3-PSP robot are solved. The governing equations of the kinematics problems of the robots are developed and embedded in the homotopy continuation function. The HCM is utilized in order to solve the nonlinear system of equations derived from the kinematics analysis of the robots. Then, to represent the real case application an initial guess far from the correct answer is selected. It is shown that, comparing with the Newton–Raphson method (NRM), the F-Kin calculation time for the Stewart robot is decreased by 43%. Therefore, using the HCM a hybrid method is suggested to solve the F-Kin of the Stewart robot. Furthermore, the HCM, as an innovative method, relieves other downsides of the conventional numerical methods, including a proper initial guess requirement as well as the problems of convergence.

Keywords Kinematics · HCM · Parallel robots · 3-PSP · Stewart platform

1 Introduction

Application of parallel robots in the industry continues to increase. These applications include simulators, cutting and welding machines, machine tools as well as CNC machines. Most of the conventional parallel robots designed to have six DOFs. However, today, with increasing application of parallel robots, the existence of parallel robots with less numbers of DOFs is also essential. These robots, besides having most of the capabilities of the parallel robots, can be manufactured with less cost. The usage of parallel robots with lower DOFs has surged in manufacturing processes due to their economic benefits [1]. In robotics, both kinematics problems (F-Kin and I-Kin problems) are essential research issues. In the case of serial manipulators, the F-Kin is easy to study, while for parallel manipulators it is the opposite. For this reason, the F-Kin of the parallel robots has been vastly investigated. This paper addresses both I-Kin and F-Kin of the parallel robots.

The Stewart parallel platform was introduced in 1965 [2]. The challenge in F-Kin of a Stewart platform is finding the positions and orientations that the end effector can reach for a given set of actuator lengths. There have been many investigations regarding the Stewart platform and its kinematics. Using the Bezout's method, Nanua et al. [3] presented a solution for the F-Kin of the Stewart platform for the first time. Zhang and Song [4] studied the geometrical condition for closed-form solutions of the F-Kin of the Stewart platforms. Liu et al. [5] proposed a simple algorithm to solve the F-Kin of the Stewart platform and derived the explicit expressions for some special configurations. In the same year, Raghavan [6] solved the F-Kin problem using a numerical technique known as polynomial continuation and showed that for Stewart platforms with general geometry this problem has 40 distinct solutions. Wampler [7] used soma coordinates to provide a simpler analytical proof of the upper bound of 40 with simple equations. Husty [8] employed the kinematic mapping method to map three dimensional kinematics to a seven-dimensional quasi-elliptic space. His algorithm ultimately led to a univariate polynomial of degree forty. Yee and Lim [9] studied the F-Kin of the Stewart platform by means of the neural networks. Dhingra et al. [10] presented an

✉ Alireza Akbarzadeh
ali_akbarzadeh@um.ac.ir

[1] Ferdowsi University of Mashhad, Mashhad, Iran

approach to F-Kin using Gröbner–Sylvester hybrid method. The following year, Ji and Wu [11] obtained a closed-form solution for the F-Kin of the Stewart platform by introducing a quaternion, also, Innocenti [12] presented an algorithm to solve the F-Kin of the general-geometry 6–6 Stewart platform in polynomial form; furthermore, using the algebraic elimination method Lee and Shim [13] considered the F-Kin of the 6–6 general Stewart platform. Gao et al. [14] proved that there exist 3850 possible forms of generalized Stewart platform and obtained closed-form solutions and the best upper bounds of real solutions of the F-Kin for a class of 1120 generalized Stewart platforms. Wang [15] presented a simple numerical method for the F-Kin of general Stewart platforms, which can generate a unique solution directly. In 2009, using Genetic Algorithms Omran et al. [16] presented a new technique for modeling the F-Kin of a Stewart platform. Huang et al. [17] studied the F-Kin of a symmetric 6–6 Stewart platform by means of the algebraic elimination algorithm. Y.H. Zhang et al. [18] analyzed the F-Kin of the Stewart platform using the Memetic Algorithms. Zhou et al. [19] proposed a new F-Kin algorithm based on dual quaternion for a general Stewart platform. Kardan and Akbarzadeh [20] proposed a new hybrid method using artificial neural networks and a third-order numerical algorithm to solve F-kin of parallel robots. Based on the literature review above, the D-Kin of the Stewart platform has been a challenging issue to be investigated since last few decades.

All above-mentioned attempts end up valuable results in the kinematics of the Stewart platform. However, to get a closed-form solution, they solve the problem by either studying the D-Kin problem with specific simplifying geometric assumptions or using computationally expensive methods with complicated mathematical definitions. Numerical approaches can be utilized to tackle these problems. In this paper, a combination of the HCM and the NRM is suggested as a fast and straightforward approach to solve the D-Kin problem of all kinds of parallel robots. This hybrid method can be used to solve highly nonlinear algebraic systems of the equations of D-Kin/I-Kin of parallel robots for all the points inside the robot's useable workspace without divergence and/or appropriate initial guess limitations.

In addition to the study of the F-Kin for the Stewart robot, in this paper, the I-Kin solution for the FUM 3-PSP parallel manipulator with 3-DOFs in space is presented. Unlike most of the parallel robots, the I-Kin of this robot, in two operational modes, is quite complicated. The FUM 3-PSP robot consists of a moving platform shaped like a symmetric tripetalous star, a fixed platform and three identical legs. Each leg makes a serial kinematic chain as Prismatic–Spherical–Prismatic (PSP), which the first P-joint in each leg is the active joint [21,22]. Inherently, the DOFs of the 3-PSP's moving platform can be classified into in non-pure coupled mixed-type motions as 1T2R. Therefore, the robot's moving platform has parasitic or uncontrollable motions. Rezaei et al. [21] presented a new general perspective to obtain the operational modes for parallel robots with lower than 6 DOFs which have non-pure DOFs. They used a methodology to select the most practical operational modes. Their methodology results in two non-pure operational modes for the FUM 3-PSP robot called "non-pure translational XYZ mode" and "non-pure coupled mixed-type $Z\theta\varphi$ mode". To solve I-Kin of the FUM 3-PSP robot, depending on each operational mode, separate solution strategies must be considered [21,22]. Obtaining analytical solutions to forward and inverse kinematics of 3-PSP are both sophisticated.

The difficulty in solving the I-Kin of the FUM 3-PSP robot depends on the selected moving platform DOFs. In [22], some numerical and analytical methods presented to solve inverse and forward kinematics of the 3-PSP parallel robot. For some operational modes, finding the analytical solution is rather difficult [22]. Therefore, a numerical approach based on the Newton iterative method employed to find a local solution. The proposed Newton's method is not computationally efficient and may not be used for real-time control. Yet, different researchers have presented methods to enhance the computation time [22,23]. Additionally, a few studies investigate the kinematics of the 3-PSP robot. Bonev [24] presented a brief discussion on obtaining the 3-PSP kinematics constraint equations. Also, Di Gregorio and Parenti-Castelli [25] solved the forward position analysis of a general 3-PSP parallel robot in analytical form using an algebraic system which has a Sylvester eliminant that is a polynomial equation of the eighth degree.

To solve the kinematics problem of the parallel manipulators, some researchers have focused on HCM as an effective method. This method, in contrast to conventional numerical methods, does not rely on a good initial guess as well as, there is almost no worry about the problem of divergence. Bin and Xiang-de [26] studied the F-Kin of a parallel robot using the continuation method, they also improved the efficiency and feasibility of the method. Abbasnejad et al. [27] utilized it in the F-Kin problem of the 3-PRS parallel manipulator, also, Varedi et al. [28] used it to study the kinematics of an offset 3-UPU translational parallel manipulator. Unlike above-mentioned papers that the HCM is used to solve the kinematics problem just for one point, in this paper a hybrid method is proposed to solve the problem for all the points of a trajectory inside the robot's useable workspace.

The paper is organized as follows. In Sect. 2, a brief introduction of the HCM is presented. Section 3 describes the ability of the HCM and the hybrid method to solve the F-Kin of the Stewart robot. In Sect. 4, using the HCM the I-Kin of the FUM 3-PSP is studied. Section 5 presents a conclusion for this study. Finally, "Appendix" section presents further explanation for some equations.

2 The homotopy continuation method

When dealing with the numerical problem, for example the NRM, there are two questions that must be answered. One is that a good initial guess is not easy to detect and another is related to if the method used will converge to useful solutions. The HCM can eliminate these shortcomings [29]. In this method a parameter, t, that assumes values in $[0, 1]$ is introduced. A problem with a known solution corresponds to $t = 0$ and the original problem corresponds to $t = 1$. A continuation method attempts to figure out the problem for $t = 1$ by solving the sequence of problems corresponding to $t_0 = 0 < t_1 < t_2 < \cdots < t_n = 1$. This method is comprised of two main parts. First, the homotopy continuation function is defined with an auxiliary homotopy function (AHF). Next, the system of nonlinear equations is solved through NRM. Consider, a system of nonlinear equations as follows,

$$\boldsymbol{F(X)} = \mathbf{0} \quad \text{i.e.,} \quad \begin{cases} f\,(x, y, \ldots, z) = 0, \\ g\,(x, y, \ldots, z) = 0, \\ \vdots \\ h\,(x, y, \ldots, z) = 0, \end{cases} \tag{1}$$

The Newton's method to solve these equations is [28],

$$\begin{bmatrix} \frac{\partial f(x_n, y_n, \ldots)}{\partial x} & \frac{\partial f(x_n, y_n, \ldots)}{\partial y} & \cdots \\ \frac{\partial g(x_n, y_n, \ldots)}{\partial x} & \frac{\partial g(x_n, y_n, \ldots)}{\partial y} & \cdots \\ \vdots & \vdots & \ddots \end{bmatrix} \begin{bmatrix} x_{n+1} - x_n \\ y_{n+1} - y_n \\ \vdots \end{bmatrix} = \begin{bmatrix} -f(x_n, y_n, \cdots) \\ -g(x_n, y_n, \cdots) \\ \vdots \end{bmatrix} \tag{2}$$

Given a set of equations in m variables $x_1, x_2, \ldots, x_m$, the equations are modified by omitting some of the terms and adding new ones until we have a new system of equations, the solutions to which may be easily guessed/given/known. Next, change the coefficients of the new system into coefficients of the original system by a series of small increments. Finally, the solution is followed through the changes, using methods such as the NRM. This is called a homotopy continuation technique. To find the solution of Eq. (1), a new simple start system is chosen and referred to as AHF [29,30],

$$\boldsymbol{G}(\boldsymbol{X}) = \mathbf{0} \tag{3}$$

The AHF $\boldsymbol{G}(\boldsymbol{X})$ must be known or controllable and easy to solve. Then, the homotopy continuation function is defined as [30],

$$\boldsymbol{H}(\boldsymbol{X}, t) \equiv t\boldsymbol{F}(\boldsymbol{X}) + (1 - t)\boldsymbol{G}(\boldsymbol{X}) = 0 \tag{4}$$

where t is the arbitrary parameter and varies from 0 to 1, i.e., $t \in [0, 1]$. Therefore, we have the following two boundary conditions [30],

$$\begin{aligned} \boldsymbol{H}(\boldsymbol{X}, 0) &= \boldsymbol{G}(\boldsymbol{X}) \\ \boldsymbol{H}(\boldsymbol{X}, 1) &= \boldsymbol{F}(\boldsymbol{X}) \end{aligned} \tag{5}$$

The goal of the method is to solve the $\boldsymbol{H}\,(\boldsymbol{X}, t) = 0$ instead of $\boldsymbol{F}\,(\boldsymbol{X}) = 0$ by varying parameter t from 0 to 1 and avoid divergence. Hence we rewrite Eq. (2) as [30],

$$\begin{bmatrix} \frac{\partial H_1(x_n, y_n, \ldots)}{\partial x} & \frac{\partial H_1(x_n, y_n, \ldots)}{\partial y} & \cdots \\ \frac{\partial H_2(x_n, y_n, \ldots)}{\partial x} & \frac{\partial H_2(x_n, y_n, \ldots)}{\partial y} & \cdots \\ \vdots & \vdots & \ddots \end{bmatrix} \begin{bmatrix} x_{n+1} - x_n \\ y_{n+1} - y_n \\ \vdots \end{bmatrix} = \begin{bmatrix} -H_1(x_n, y_n, \cdots) \\ -H_2(x_n, y_n, \cdots) \\ \vdots \end{bmatrix} \tag{6}$$

To avoid divergence, Wu [31] provided some useful choices of the AHF. They can be in the form of polynomial, harmonic, exponential, or any of their combinations. By appropriately choosing/adjusting the AHF, we can obtain the solutions of Eq. (1) [30].

3 Case study 1: kinematics model of the Stewart platform

Stewart platforms are constructed of two platforms connected to each other through six extendable legs. In this paper, a 6–3 UPS (Universal, Prismatic, Spherical) Stewart parallel manipulator, illustrated in Fig. 1a, is studied. For this structure, the upper platform (moving part) is a triangle where each of its vertices is connected to two legs of the robot through a compound spherical joint. The compound spherical joint is designed to have six rotational DOFs, see Fig. 1b. In this design, two revolute joints ($j + 2$ and $j + 3$) are common for the ith and $i + 1$th legs. The other end of each leg is attached to a universal joint which itself is connected to the base platform. Each leg has an actuated prismatic joint. However, unlike the top platform, the base is a hexagon. The mechanism appeared in Fig. 1 can be represented by the equivalent mechanism in Fig. 2a. The hypothetical mechanism including three kinematics length, O_1T_1, O_2T_2, and O_3T_3, is kinematically equivalent to the six leg Stewart platform of Fig. 1 [3]. The linkage $B_1T_1B_2$ can be replaced by a single link with a revolute joint at one end and a spherical joint at the other end. The revolute joint will lie on the intersection of the line joining B_1 and B_2 and the line passing through T_1 and normal to the line B_1B_2. The direction of the joint axis will also be along B_1B_2. Thus, the linkages $B_1T_1B_2$,

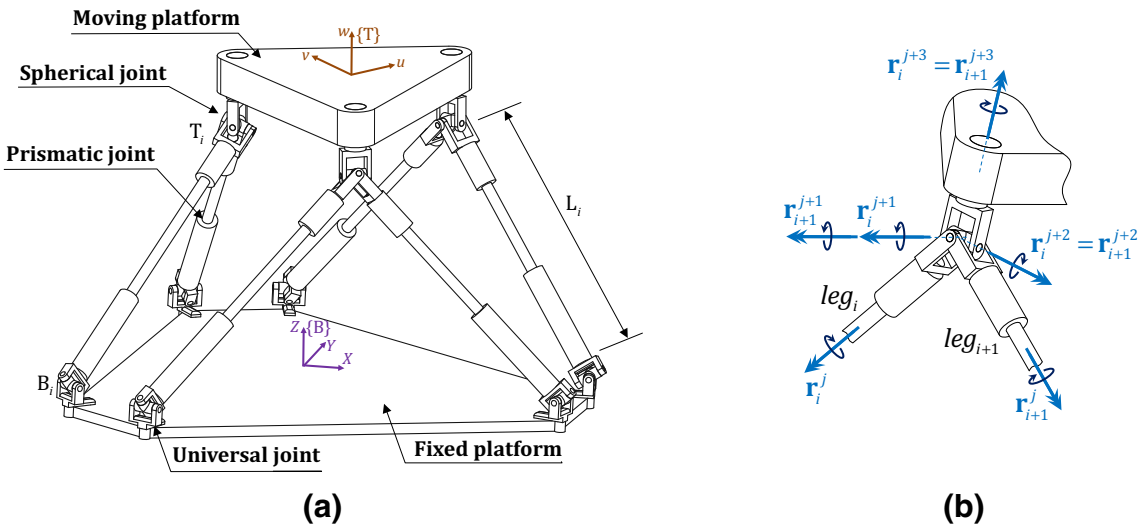

Fig. 1 Scheme of the 6–3 Stewart parallel manipulator

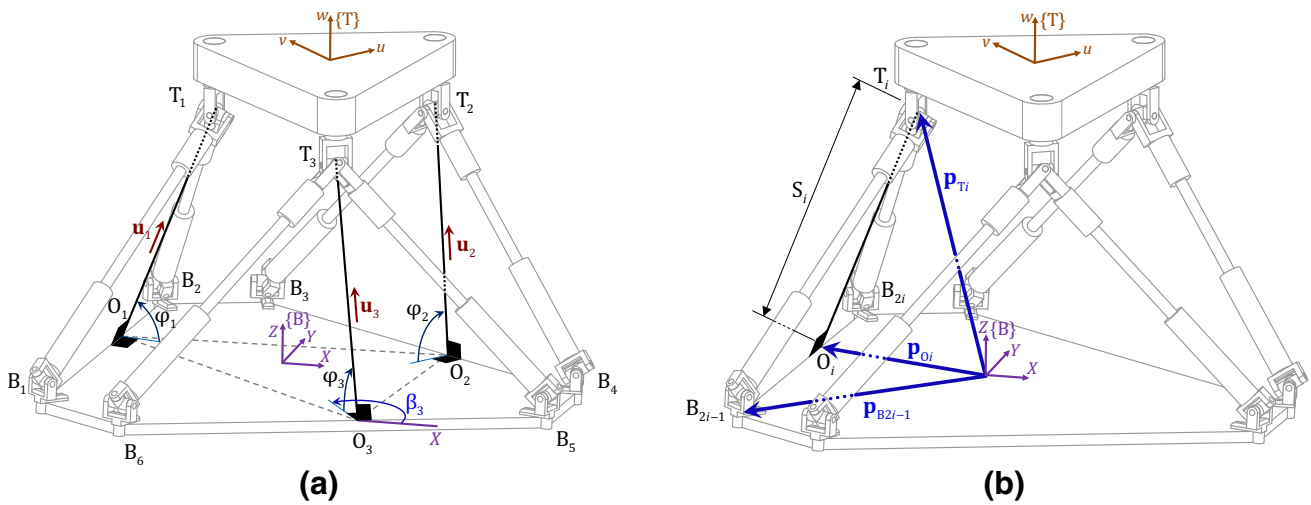

Fig. 2 Equivalent mechanism for the 6–3 Stewart platform and position vectors

$B_3T_2B_4$, and $B_5T_3B_6$ can be replaced by links O_1T_1, O_2T_2, and O_3T_3, respectively [3].

3.1 Kinematic constraint equations

In this study, the lower index "i" represents $i = 1, 2, 3$. To determine the locations of O_i we need to find the lengths t_{i1}. Where t_{i1} is the distance between B_{2i-1} and O_i. S_i and t_{i1} must be defined in terms of the leg lengths $L_1, \ldots, L_6$. Consider Fig. 2a, if the lengths of $B_{2i-1}B_{2i}$ are equivalent to fixed values of a_i, then,

$$t_{i1} = \frac{a_i^2 + L_{2i-1}^2 - L_{2i}^2}{2a_i}; \quad t_{i2} = a_i - t_{i1} \tag{7}$$

$$S_i = \sqrt{L_{2i-1}^2 - t_{i1}^2} \tag{8}$$

The inertia frame $B\{X, Y, Z\}$ is fixed to the base platform with its XY axis lying in the plane of the base platform. Then, the position vectors of O_i can be written as follows (Fig. 2b),

$$\mathbf{p}_{O_i} = \mathbf{p}_{B_{2i-1}} + t_{i1}\frac{(\mathbf{p}_{B_{2i}} - \mathbf{p}_{B_{2i-1}})}{|\mathbf{p}_{B_{2i}} - \mathbf{p}_{B_{2i-1}}|} \tag{9}$$

Moreover, β_i, the angles made by the lines perpendicular to $B_{2i-1}B_{2i}$ with the X axis are given by the following equations,

$$\begin{aligned}\beta_i &= \cos^{-1}\left[\frac{\{(\mathbf{p}_{B_{2i}} - \mathbf{p}_{B_{2i-1}}) \times \mathbf{k}\} \cdot \mathbf{i}}{|(\mathbf{p}_{B_{2i}} - \mathbf{p}_{B_{2i-1}}) \times \mathbf{k}|}\right] \\ &= \sin^{-1}\left[\frac{\{(\mathbf{p}_{B_{2i}} - \mathbf{p}_{B_{2i-1}}) \times \mathbf{k}\} \cdot \mathbf{j}}{|(\mathbf{p}_{B_{2i}} - \mathbf{p}_{B_{2i-1}}) \times \mathbf{k}|}\right]\end{aligned} \tag{10}$$

where $\boldsymbol{i}, \boldsymbol{j}$, and $\boldsymbol{k}$ are unit vectors along X, Y, and Z axes of the inertia frame. Considering Fig. 2a and the definition of β angles, the unit vectors $\mathbf{u}_i$, along O_iT_i, can be given by following equations,

$$\mathbf{u}_i = \cos\beta_i \cos\varphi_i \mathbf{i} + \sin\beta_i \cos\varphi_i \mathbf{j} + \sin\varphi_i \mathbf{k} \tag{11}$$

Next, define the position vectors for T_i as,

$$\mathbf{p}_{T_i} = \mathbf{p}_{O_i} + S_i \mathbf{u}_i \tag{12}$$

There are constant distances between T_1, T_2, and T_3. In the event that the lengths of T_1T_3, T_2T_3, and T_1T_2 are equal to the values of d, e, and f, respectively, we can write,

$$\left|\mathbf{p}_{T_3} - \mathbf{p}_{T_1}\right|^2 = d^2 \tag{13}$$

$$\left|\mathbf{p}_{T_3} - \mathbf{p}_{T_2}\right|^2 = e^2 \tag{14}$$

$$\left|\mathbf{p}_{T_2} - \mathbf{p}_{T_1}\right|^2 = f^2 \tag{15}$$

3.2 Solution procedure

Substitution of Eqs. (12) in (13) results in,

$$\begin{aligned}&\left((\mathbf{p}_{O_3})_X - (\mathbf{p}_{O_1})_X + S_3\cos\beta_3\cos\varphi_3 - S_1\cos\beta_1\cos\varphi_1\right)^2\\&+\left((\mathbf{p}_{O_3})_Y - (\mathbf{p}_{O_1})_Y + S_3\sin\beta_3\cos\varphi_3 - S_1\sin\beta_1\cos\varphi_1\right)^2\\&+(S_3\sin\varphi_3 - S_1\sin\varphi_1)^2 = d^2\end{aligned} \tag{16}$$

With some simplification, following equation is obtained,

$$\begin{aligned}&E_1\cos\varphi_1 + E_2\cos\varphi_3 + E_3\cos\varphi_1 cos\varphi_3\\&+E_4\sin\varphi_1\sin\varphi_3 + E_5 = 0\end{aligned} \tag{17}$$

where

$$\begin{aligned}E_1 &= 2S_1\cos\beta_1\left\{(\mathbf{p}_{O_1})_X - (\mathbf{p}_{O_3})_X\right\}\\&\quad+2S_1\sin\beta_1\left\{(\mathbf{p}_{O_1})_Y - (\mathbf{p}_{O_3})_Y\right\}\\E_2 &= -2S_3\cos\beta_3\left\{(\mathbf{p}_{O_1})_X - (\mathbf{p}_{O_3})_X\right\}\\&\quad-2S_3\sin\beta_3\left\{(\mathbf{p}_{O_1})_Y - (\mathbf{p}_{O_3})_Y\right\}\\E_3 &= -2S_1S_3\cos(\beta_1-\beta_3)\\E_4 &= -2S_1S_3\\E_5 &= \left((\mathbf{p}_{O_3})_X - (\mathbf{p}_{O_1})_X\right)^2 + \left((\mathbf{p}_{O_3})_Y - (\mathbf{p}_{O_1})_Y\right)^2\\&\quad+S_1^2 + S_3^2 - d^2\end{aligned} \tag{18}$$

The same procedure is implemented on Eqs. (14) and (15). Then, substitution of Eq. (12) in (14) results in,

$$\begin{aligned}&H_1\cos\varphi_3 + H_2\cos\varphi_2 + H_3\cos\varphi_2\cos\varphi_3\\&+H_4\sin\varphi_2\sin\varphi_3 + H_5 = 0\end{aligned} \tag{19}$$

where

$$\begin{aligned}H_1 &= 2S_3\cos\beta_3\left\{(\mathbf{p}_{O_3})_X - (\mathbf{p}_{O_2})_X\right\}\\&\quad+2S_3\sin\beta_3\left\{(\mathbf{p}_{O_3})_Y - (\mathbf{p}_{O_2})_Y\right\}\\H_2 &= -2S_2\cos\beta_2\left\{(\mathbf{p}_{O_3})_X - (\mathbf{p}_{O_2})_X\right\}\\&\quad-2S_2\sin\beta_2\left\{(\mathbf{p}_{O_3})_Y - (\mathbf{p}_{O_2})_Y\right\}\\H_3 &= -2S_2S_3\cos(\beta_3-\beta_2)\\H_4 &= -2S_2S_3\\H_5 &= \left((\mathbf{p}_{O_3})_X - (\mathbf{p}_{O_2})_X\right)^2 + \left((\mathbf{p}_{O_3})_Y - (\mathbf{p}_{O_2})_Y\right)^2\\&\quad+S_2^2 + S_3^2 - e^2\end{aligned} \tag{20}$$

Moreover, substitution of Eq. (12) in (15) results in,

$$\begin{aligned}&I_1\cos\varphi_2 + I_2\cos\varphi_1 + I_3\cos\varphi_1\cos\varphi_2\\&+I_4\sin\varphi_1\sin\varphi_2 + I_5 = 0\end{aligned} \tag{21}$$

where

$$\begin{aligned}I_1 &= 2S_2\cos\beta_2\left\{(\mathbf{p}_{O_2})_X - (\mathbf{p}_{O_1})_X\right\}\\&\quad+2S_2\sin\beta_2\left\{(\mathbf{p}_{O_2})_Y - (\mathbf{p}_{O_1})_Y\right\}\\I_2 &= -2S_1\cos\beta_1\left\{(\mathbf{p}_{O_2})_X - (\mathbf{p}_{O_1})_X\right\}\\&\quad-2S_1\sin\beta_1\left\{(\mathbf{p}_{O_2})_Y - (\mathbf{p}_{O_1})_Y\right\}\\I_3 &= -2S_1S_2\cos(\beta_2-\beta_1)\\I_4 &= -2S_1\ S_2\\I_5 &= \left((\mathbf{p}_{O_2})_X - (\mathbf{p}_{O_1})_X\right)^2 + \left((\mathbf{p}_{O_2})_Y - (\mathbf{p}_{O_1})_Y\right)^2\\&\quad+S_1^2 + S_2^2 - f^2\end{aligned} \tag{22}$$

For the Sines and Cosines angles used in Eqs. (17), (19), and (21) the following equivalent algebraic expressions are substituted,

$$\sin\varphi_i = \frac{2x_i}{1+x_i^2}, \quad \cos\varphi_i = \frac{1-x_i^2}{1+x_i^2} \tag{23}$$

where $x_i = \tan\left(\frac{\varphi_i}{2}\right)$. Upon simplification the following equations are derived,

$$\left(J_1x_1^2 + J_2\right)x_3^2 + (J_3x_1)\,x_3 + \left(J_4x_1^2 + J_5\right) = 0 \tag{24}$$

$$\left(K_1x_2^2 + K_4\right)x_3^2 + (K_3x_2)\,x_3 + \left(K_2x_2^2 + K_5\right) = 0 \tag{25}$$

$$\left(M_1x_1^2 + M_4\right)x_2^2 + (M_3x_1)\,x_2 + \left(M_2x_1^2 + M_5\right) = 0 \tag{26}$$

where

$$J_1 = E_3 - E_1 - E_2 + E_5$$

$$J_2 = E_1 - E_2 - E_3 + E_5$$

Table 1 Geometric parameters of the manipulator and coordinates of the base platform

Legs' lengths	$L_1(m)$	$L_2(m)$	$L_3(m)$	$L_4(m)$	$L_5(m)$	$L_6(m)$
Values	5	4.5	5.5	5	5.7	5.5
Coordinates of B_i	$\mathbf{p}_{B_1}$	$\mathbf{p}_{B_2}$	$\mathbf{p}_{B_3}$	$\mathbf{p}_{B_4}$	$\mathbf{p}_{B_5}$	$\mathbf{p}_{B_6}$
Values	[−2.9, −0.9, 0]	[−1.2, 3.0, 0]	[2.5, 4.1, 0]	[3.2, 1.0, 0]	[1.3, −2.3, 0]	[−1.2, −3.7, 0]

$$J_3 = 4E_4$$
$$J_4 = E_2 - E_1 - E_3 + E_5$$
$$J_5 = E_1 + E_2 + E_3 + E_5 \tag{27}$$

In Eqs. (25) and (26), the K's and M's are the same as J's with the E's replaced by the corresponding H's and I's, respectively. This results in a system of nonlinear equations in three variables x_1, x_2, and x_3, i.e., Eqs. (24)–(26). This system of nonlinear equations can be solved through the use of the HCM. To verify the results of the HCM, physical dimensions of the robot are considered as given in [3], i.e., $d = 3m$ and $e = f = 2m$. Additionally, the geometric parameters of the manipulator and coordinates of the base platform are shown in Table 1.

Substitution of the parameters from Table 1 into Eqs. (24)–(26) yields,

$$179.97627x_1^2x_3^2 + 1.61638x_1^2 - 182.21613x_1x_3 + 51.61314x_3^2 + 18.39595 = 0 \tag{28}$$
$$141.55158x_2^2x_3^2 + 113.96639x_2^2 - 213.48715x_2x_3 + 86.35768x_3^2 - 1.94854 = 0 \tag{29}$$
$$179.64468x_1^2x_2^2 + 17.96356x_1^2 - 166.72890x_1x_2 + 38.52657x_2^2 + 11.25726 = 0 \tag{30}$$

The homotopy continuation functions are as follows,

$$\left[179.97627x_1^2x_3^2 + 1.61638x_1^2 - 182.21613x_1x_3 + 51.61314x_3^2 + 18.39595\right] \times t + (1-t) \times G_1 = 0 \tag{31}$$
$$\left[141.55158x_2^2x_3^2 + 113.96639x_2^2 - 213.48715x_2x_3 + 86.35768x_3^2 - 1.94854\right] \times t + (1-t) \times G_2 = 0 \tag{32}$$
$$\left[179.64468x_1^2x_2^2 + 17.96356x_1^2 - 166.72890x_1x_2 + 38.52657x_2^2 + 11.25726\right] \times t + (1-t) \times G_3 = 0 \tag{33}$$

Equations (31)–(33) must be solved simultaneously to solve the F-Kin to obtain x_1, x_2 and x_3 values. Once x_1, x_2 and x_3 are given, $\mathbf{u}_i$ are defined by Eq. (11). Then, the positions of T_i relative to the fixed frame are uniquely determined by Eq. (12). To do this, using the steps of 0.01, the homotopy parameter, t, changes from 0 to 1. The initial guesses used for all three unknown parameters are equal to 1, i.e., $(x_1, x_2, x_3) = (1, 1, 1)$. Using the NRM, the set of Eqs. (31)–(33) are solved by changing the combination of the AHFs, the G_i. Table 2 shows the AHFs and their results.

Table 2 The AHFs and their results

AHFs	Outputs (x_1, x_2, x_3)
$(-3x_1, x_2, x_3)$	(−0.96425, −0.26103, −0.13646)
$(-x_1, -x_2, -x_3)$	(0.44266, 0.27671, 0.45428)
(x_1, x_2, x_3)	(−0.44266, −0.27671, −0.45428)
$(3x_1, -x_2, -x_3)$	(0.96425, 0.26103, 0.13646)

Taking into account Eq. (23), the values of φ_i are uniquely determined in the interval $0 < \varphi_i < 360$. These values are shown in Table 3. The angles in this table are in degrees. Results of the F-Kin of the Stewart platform in Table 3 and those reported by Nanua et al. [3] are unanimous. It is worth mentioning that, more different forms, values, and functions of the AHFs lead to repetitive results, as illustrated in Table 4. Moreover, although different AHFs are used in Table 4, there is no significant difference in elapsed times.

Table 3 Four real solutions of the sample Stewart platform

(x_1, x_2, x_3)	$(\varphi_1, \varphi_2, \varphi_3)$
(−0.96425, −0.26103, −0.13646)	(−87.9145, −29.2588, −15.5409)
(0.44266, 0.27671, 0.45428)	(47.7537, 30.9349, 48.8631)
(−0.44266, −0.27671, −0.45428)	(−47.7537, −30.9349, −48.8631)
(0.96425, 0.26103, 0.13646)	(87.9145, 29.2588, 15.5409)

Table 4 AHFs which result in the same answers

AHFs	Outputs (x_1, x_2, x_3)	Elapsed time (s)
$(x_1, -x_2, -x_3)$	(−0.44266, −0.27671, −0.45428)	2.854700
$(x_1, -x_2, x_3)$	(−0.44266, −0.27671, −0.45428)	2.856012
$(x_1, -x_2 - 1, x_3)$	(−0.44266, −0.27671, −0.45428)	2.858512
$(x_1, x_2 - 2, x_3)$	(−0.44266, −0.27671, −0.45428)	2.845479

Table 5 Initial guesses which result in the same answers

Initial guesses	Outputs (x_1, x_2, x_3)	Elapsed time (s)
$(-1, -1, -1)$	$(-0.44266, -0.27671, -0.45428)$	2.879284
$(1, 10, 100)$	$(-0.44266, -0.27671, -0.45428)$	2.893191
$(-50, -100, -150)$	$(-0.44266, -0.27671, -0.45428)$	2.888375
$(100, 200, 300)$	$(-0.44266, -0.27671, -0.45428)$	2.879405

Furthermore, with a certain set of AHFs, e.g., (x_1, x_2, x_3), the results are not affected significantly by changing initial guesses of the unknown parameters. This is illustrated in Table 5.

In addition, it is obvious that the larger increments imply slower solution algorithm. In other words, using the steps of 0.001 or 0.0001, rather than 0.01, results in a significant increase in the HCM computation time. Table 6 shows a comparison between the NRM and the HCM speeds; the step length for the HCM is equal to 0.01. As shown in this table, when the initial guesses are far from the actual answers, the HCM is faster. However, for the initial guesses near the actual answers there is no significant change in the elapsed time for the HCM, while the NRM experiences a rather large drop in the elapsed time. It should be noted that it is not realistic to expect to have good initial guess which, therefore, shows the superiority of the HCM in this case.

Therefore, based on the results in Table 6, it can be concluded that the HCM has better performance when the initial guess is not close to the real solution, while the NRM is superior in cases that a good initial guess is available. To use both these characteristics simultaneously, a combined method is suggested to solve the F-Kin of the Stewart platform. For a given joint-space trajectory, it is more computationally efficient to use both the HCM and the NRM. To do this, the HCM is used to find the answer for the initial point. For the second point, the answer found by HCM for the first point can be used as the initial guess for the NRM method. For all remaining points, the NRM is used where the previous point answer is used as the initial guess for the NRM.

4 Case study 2: kinematics model of the 3-PSP parallel manipulator

In this section, position analysis of a specific architecture of a 3-PSP parallel manipulator is investigated. Unlike serial manipulators, commonly the I-Kin solution of parallel robots has a closed form. However, obtaining the I-Kin solution of the 3-PSP is difficult, and therefore numerical methods are employed. This makes the 3-PSP a good candidate for using the HCM method.

The 3-PSP robot is a 3-DOFs fully parallel mechanism comprised of a fixed platform including two parts (bottom and top) and a symmetric planar tripetalous moving platform which is called Moving Star, MS, see Fig. 3b. It is noted that various tools can be located on the MS center. The MS and the fixed platform are connected through three identical parallel legs. Each leg is a Prismatic–Spherical–Prismatic, PSP, serial kinematic chain and its first P-joint is the active joint (see [21, 22] for more details). Figure 3a shows a serial kinematic chain of a general 3-PSP parallel robot. Furthermore, in Fig. 3b, the FUM 3-PSP parallel robot is shown. In this case study, dimensional parameters l_i, c_i, and d_i are all assumed to be zero, which insures an intersection in the axis of the passive prismatic and spherical joints.

4.1 Identification of the operational modes and vectors description

Coordinate frames and vectors of the FUM 3-PSP parallel manipulator are shown in Fig. 4. A fixed coordinate frame $B\{x, y, z\}$ is embedded at point O on top fixed triangle $\Delta A_1A_2A_3$ and moving coordinate frame $T\{u, v, w\}$ is embedded at point T, which is the MS center. It is noted that a leading superscript shows the coordinate frame in which the vector is referenced. The superscript "B" indicating frame $\{B\}$ in which vectors are defined is eliminated to be brief. Vector $\mathbf{a}_i$ locate corner of A_i in $\{B\}$, vector $\mathbf{q}_i^{ac}$ specify length of linear rods (LR), vector ${}^{T}\mathbf{b}_i$ connects point T to the ith S-joint, S_i, and vector ${}^{T}\mathbf{h}$ connects point T to point P in

Table 6 Comparison between the speed of convergence in HCM and NRM

Initial guesses	AHFs	Outputs (x_1, x_2, x_3)	Elapsed time (s)		Elapsed time changes by HCM (%)
			NRM	HCM	
$(-5, -10, -15)$	(x_1, x_2, x_3)	$(-0.44266, -0.27671, -0.45428)$	4.929761	2.773881	−43.7319
$(5, 10, 15)$	$(-x_1, x_2, x_3)$	$(0.44266, 0.27671, 0.45428)$	5.064923	2.845260	−43.8242
$(-1, -1, -1)$	(x_1, x_2, x_3)	$(-0.44266, -0.27671, -0.45428)$	5.047875	2.871802	−43.1087
$(1, 1, 1)$	$(-x_1, x_2, x_3)$	$(0.44266, 0.27671, 0.45428)$	5.093762	2.843005	−44.1865
$(-0.4, -0.3, -0.5)$	(x_1, x_2, x_3)	$(-0.44266, -0.27671, -0.45428)$	1.202943	2.745923	+128.2671
$(0.4, 0.3, 0.5)$	$(-x_1, x_2, x_3)$	$(0.44266, 0.27671, 0.45428)$	1.195136	2.795026	+133.8668

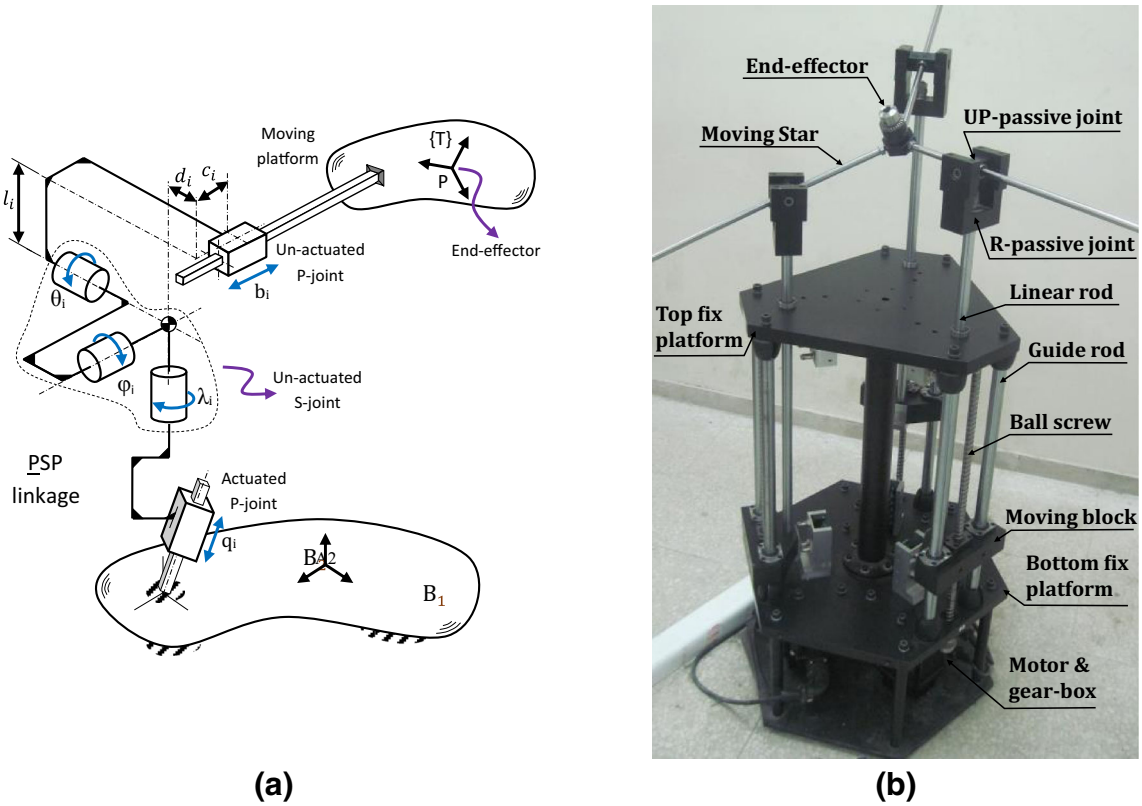

Fig. 3 **a** A kinematic chain of a general 3-PSP robot, **b** a simplified equivalent form of the spatial FUM 3-PSP parallel manipulator

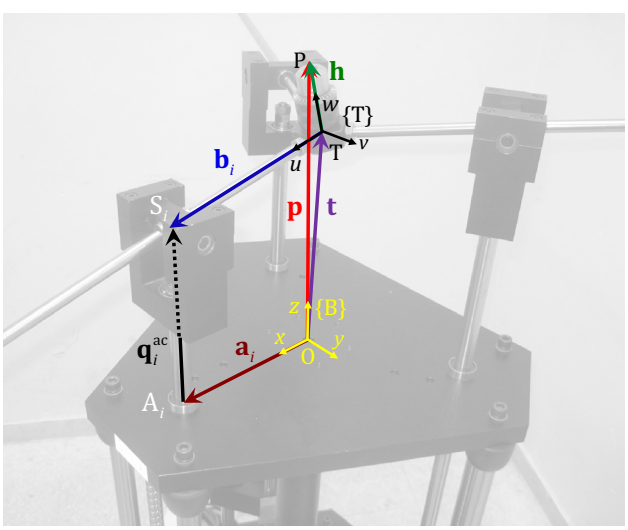

Fig. 4 The vectors and coordinate frames for a typical kinematic chain of the FUM 3-PSP parallel robot

$\{T\}$. Vectors $\mathbf{t} = \{x_T, y_T, z_T\}^T$ and $\mathbf{p} = \{x_P, y_P, z_P\}^T$ denote point T, the end-effector position, and point P, the tool tip, respectively.

A classification for the 3-DOFs spatial parallel robots is presented in [21]. In this classification, the DOFs of the 3-PSP's moving platform can be inherently classified into non-pure coupled mixed-type motions as 1T2R. Therefore, the robot's moving platform has parasitic or uncontrollable motions. Rezaei et al. [22] presented a methodology to select the most practical operational modes for the parallel robots with lower than 6-DOFs which have non-pure DOFs. In particular, for the 3-PSP parallel robot, two non-pure operational modes are obtained called "non-pure translational XYZ mode" and "non-pure coupled mixed-type $Z\theta\varphi$ mode" [22]. It is worth noting that for each operational mode a different method must be employed to evaluate the inverse kinematic [21,22]. For some operational modes, finding the analytical solution is rather difficult [21]. Therefore, numerical methods are utilized in order to find a local solution.

Figure 5 illustrates the procedure chart for the I-Kin of the FUM 3-PSP parallel manipulator in its two most practical operational modes.

4.2 I-Kin analysis

The degrees of freedom of a parallel robot are equivalent to its moving platform independent motion variables number. Thus, for the FUM 3-PSP parallel robot with 3-DOFs in space, only three motion variables of the total six MS motion variables are independent and controllable. This principle makes the concept of the operational modes in parallel robot

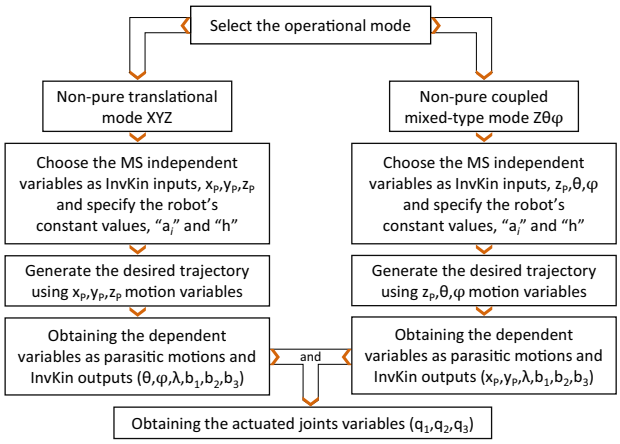

Fig. 5 I-Kin process diagram for the FUM 3-PSP parallel manipulator

with lower than 6-DOFs. As stated earlier, two operational modes called non-pure translational XYZ mode and non-pure coupled mixed-type $Z\theta\varphi$ mode are considered for the inverse position analysis. As depicted in Fig. 5, depending on the selected operational mode, separate solution strategy to solve the I-Kin problem can be considered (see [21,22] for more details). Since the FUM 3-PSP has a symmetric structure, there are three algebraically similar constraint equations. Considering Fig. 4, three closed-loop vector equations can be written as follows,

$$\mathbf{a}_i + \mathbf{q}_i^{\mathrm{ac}} = {}^{\mathrm{B}}_{\mathrm{T}}\mathbf{R}\left({}^{\mathrm{T}}\mathbf{b}_i - {}^{\mathrm{T}}\mathbf{h}\right) = \mathbf{p} \tag{34}$$

where ${}^{\mathrm{B}}_{\mathrm{T}}\mathbf{R}$ is a rotation matrix to transfer a vector defined in $\{T\}$ to $\{B\}$. These constraint equations consist of 3 vector equations which are nine nonlinear algebraic equations as $\boldsymbol{\psi}_{9\times1}(\mathbf{q}_{12\times1}) = \mathbf{0}_{9\times1}$. The general coordinates used for kinematics modeling of the robot are,

$$\begin{aligned} q_{12\times1} &= \left\{ q_{3\times1}^{\mathrm{ac}} \; q_{9\times1}^{\text{un-ac}} \right\} \\ &= \left\{ \underbrace{q_1^{\mathrm{ac}}, q_2^{\mathrm{ac}}, q_3^{ac}}_{\text{ac.}} \; \underbrace{x_{\mathrm{p}}, y_{\mathrm{p}}, z_{\mathrm{p}}, \theta, \varphi, \lambda, b_1, b_2, b_3}_{\text{Un-ac.}} \right\}^{\mathrm{T}} \end{aligned} \tag{35}$$

where $\mathbf{q}_{3\times1}^{\mathrm{ac}}$ and $\mathbf{q}_{9\times1}^{\text{un-ac}}$ are vectors of actuated and un-actuated variables, respectively. The set of constraint equations, $\boldsymbol{\psi}(\mathbf{q}) = \mathbf{0}$, which is shown in "Appendix" section , are extracted from Eq. (34). In this paper, the HCM is utilized to solve the nonlinear system of equations derived from closed vector-loop equations of the FUM 3-PSP robot. To do this, two operational modes are considered and the HCM is used to obtain the solutions. The I-Kin for both with and without considering the tool length in each operational mode is solved. While the tool length is considered, it is $h = 8$ cm.

4.2.1 I-Kin for non-pure coupled mixed-type mode $Z\theta\varphi$

In this problem, three motion variables Z, θ and φ of the MS are considered as independent variables. Consequently, these variables are the inputs of the I-Kin problem. Therefore, the three motion variables x, y, and λ are dependent on the independent motion variables of Z, θ and φ. Eliminating b_i and q_i from Eq. (39), see the "Appendix" section, as well as substituting $\sin\lambda = \frac{2x_3}{1+x_3^2}$ and $\cos\lambda = \frac{1-x_3^2}{1+x_3^2}$ where $x_3 = \tan\left(\frac{\lambda}{2}\right)$ will result in three equations. These equations for I-Kin input values $\theta = -35.01°$, $\varphi = 0°$ and $z_{\mathrm{p}} = 0.25(m)$ are as follows,

$$\begin{aligned} &0.573719h - y_{\mathrm{p}} - 2ax_3 + 2x_3x_{\mathrm{p}} + 0.573719hx_3^2 + x_3^2y_{\mathrm{p}} = 0 \\ &0.542844a + 1.987422h - 4.914311x_{\mathrm{p}} - 3.464102y_{\mathrm{p}} \\ &\quad + 11.975939ax_3 + 6.928203x_3x_{\mathrm{p}} - 9.828623x_3y_{\mathrm{p}} \\ &\quad - 0.542844ax_3^2 + 1.987422hx_3^2 + 4.914311x_3^2x_{\mathrm{p}} \\ &\quad + 3.464102x_3^2y_{\mathrm{p}} = 0 \\ &1.987422h - 0.542844a + 4.914311x_{\mathrm{p}} - 3.464102y_{\mathrm{p}} \\ &\quad + 11.975939ax_3 + 6.928203x_3x_{\mathrm{p}} + 9.828623x_3y_{\mathrm{p}} \\ &\quad + 0.542844ax_3^2 + 1.987422hx_3^2 - 4.914311x_3^2x_{\mathrm{p}} \\ &\quad + 3.464102x_3^2y_{\mathrm{p}} = 0 \end{aligned} \tag{36}$$

Then, the homotopy continuation function can be written as follows,

$$\begin{aligned} &\left[0.573719h - y_{\mathrm{p}} - 2ax_3 + 2x_3x_{\mathrm{p}} + 0.573719hx_3^2 + x_3^2y_{\mathrm{p}}\right] \\ &\quad \times t + (1-t) \times G_1 = 0 \\ &\left[0.542844a + 1.987422h - 4.914311x_{\mathrm{p}} - 3.464102y_{\mathrm{p}}\right. \\ &\quad + 11.975939ax_3 + 6.928203x_3x_{\mathrm{p}} - 9.828623x_3y_{\mathrm{p}} \\ &\quad - 0.542844ax_3^2 + 1.987422hx_3^2 + 4.914311x_3^2x_{\mathrm{p}} \\ &\quad \left. + 3.464102x_3^2y_{\mathrm{p}}\right] \times t + (1-t) \times G_2 = 0 \\ &\left[1.987422h - 0.542844a + 4.914311x_{\mathrm{p}} - 3.464102y_{\mathrm{p}}\right. \\ &\quad + 11.975939ax_3 + 6.928203x_3x_{\mathrm{p}} + 9.828623x_3y_{\mathrm{p}} \\ &\quad + 0.542844ax_3^2 + 1.987422hx_3^2 - 4.914311x_3^2x_{\mathrm{p}} \\ &\quad \left. + 3.464102x_3^2y_{\mathrm{p}}\right] \times t + (1-t) \times G_3 = 0 \end{aligned} \tag{37}$$

Next, with the steps of 0.0001, the homotopy parameter, t, changes from 0 to 1. The initial guesses used for all three unknown parameters are equal to 1, i.e., $(x_{\mathrm{p}}, y_{\mathrm{p}}, x_3) = (1, 1, 1)$. Using the NRM, the set of Eq. (37) are solved. The AHFs and their results are shown in Table 7 and Fig. 6. To provide a better visual perspective, the tool position at $\theta = 0$, $\varphi = 0$ and $z_{\mathrm{p}} = 0.25(m)$ is also shown in Fig. 6. Taking into account $x_3 = \tan\left(\frac{\lambda}{2}\right)$, the value of λ is uniquely determined in the interval $0 < \lambda < 360°$.

Table 7 The AHFs and their results for operational mode $Z\theta\phi$

	AHFs	Outputs									
	(G_1, G_2, G_3)	$x_P(m)$	$y_P(m)$	x_3	$\lambda°$	$q_1(m)$	$q_2(m)$	$q_3(m)$	$b_1(m)$	$b_2(m)$	$b_3(m)$
Case#1	(x_p, y_p, x_3)	**0.02**	**0**	0	0	0.2500	0.1402	0.3598	0.1610	0.2210	0.2210
Case#2	(x_p, y_p, x_3)	0.02	0.046	0	0	0.1845	0.0747	0.2943	0.1610	0.2210	0.2210

I-Kin input values: $\theta = -\mathbf{35.01}°$, $\varphi = \mathbf{0}°$ and $z_p = \mathbf{0.25}(m)$
Case#1: $a = 0.181(m)$, $h = 0(m)$
Case#2: $a = 0.181\ (m)$, $h = 0.08(m)$

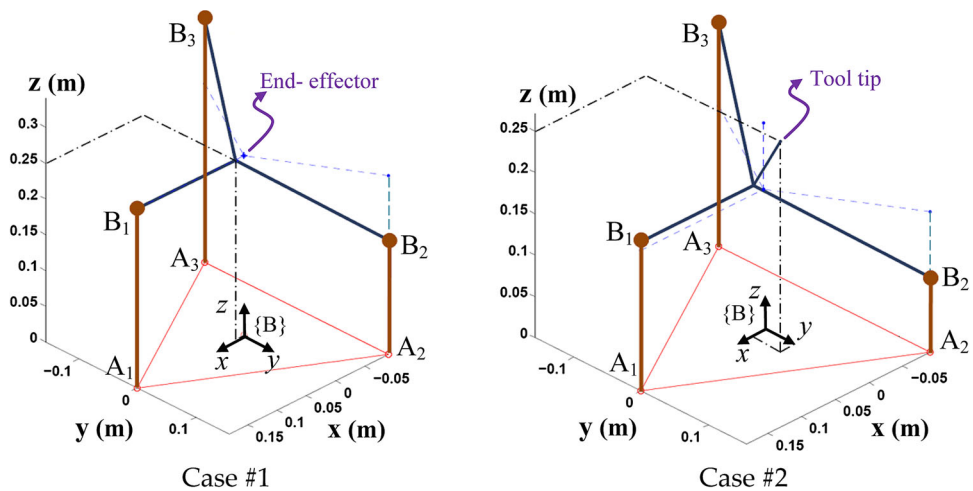

Fig. 6 I-Kin results for mode $Z\theta\varphi$

4.2.2 I-Kin for non-pure translational mode XYZ

In this problem, three motion variables X, Y, and Z of the MS are considered as independent variables. Consequently, these variables are the inputs of the I-Kin problem. Therefore, the three motion variables θ, φ, and λ are dependent on independent motion variables of X, Y and Z. Eliminating b_i and q_i from Eq. (40) as well as substituting $\sin\varphi_i = \frac{2x_i}{1+x_i^2}$ and $\cos\varphi_i = \frac{1-x_i^2}{1+x_i^2}$ where $x_i = \tan\left(\frac{\varphi_i}{2}\right)$, $\varphi_1 = \theta$, $\varphi_2 = \varphi$, and $\varphi_3 = \lambda$, will result in three equations. Finally, for I-Kin input values $x_p = 0.02(m)$, $y_p = 0$, and $z_p = 0.25(m)$ three equations can be obtained, for more details see (41). Based on Eq. (41), the homotopy continuation function can be written as Eq. (38). Next, with the steps of 0.0001, the homotopy parameter, t, changes from 0 to 1. The initial guesses used for all three unknown parameters are equal to 1, i.e., $(x_p, y_p, x_3) = (1, 1, 1)$. Using the NRM, the set of Eq. (38) are solved. The AHFs and their results are depicted in Fig. 7 and Table 8. The selected XYZ input position is equal to the output of the $Z\theta\varphi$ shown in Table 7—Case#1.

$$\left[x_3 - 50ax_3 - 50hx_1 + x_1^2x_3 - 50ax_1^2x_3 - 50hx_1x_3^2\right] \times t + (1-t) \times G_1 = 0$$

$$\begin{aligned}
&\Big[3x_1 + 1.732x_2 + 3x_1^3x_3^2 + 3x_1^3x_2^4 - 1.732x_1^4x_2^3 \\
&-1.732x_2^3x_3^2 - 3.464x_1x_3 - 2x_2x_3 - 150ax_1^3 \\
&+86.602ax_2^3 + 173.205hx_1^2 - 173.205hx_2^2 \\
&-3x_1x_3^2 - 3x_1x_2^4 - 1.732x_2x_3^2 - 3.464x_1^3x_3 \\
&-1.732x_1^4x_2 + 2x_2^3x_3 - 3x_1^3 + 1.732x_2^3 + 450ax_1x_2^2 \\
&+433.013ax_1^2x_2 - 150ax_1x_2^4 + 173.205ax_1^3x_3 \\
&-86.602ax_1^4x_2 - 100ax_2^3x_3 + 200hx_1x_2^3 - 200hx_1^3x_2 \\
&+20.785x_1x_2^2x_3 + 20x_1^2x_2x_3 - 3.464x_1x_2^4x_3 - 2x_1^4x_2x_3 \\
&-433.013ax_1^2x_2^3 + 450ax_1^3x_2^2 + 150ax_1^3x_3^2 \\
&-86.602ax_2^3x_3^2 - 692.82hx_1^2x_2^2 + 173.205hx_1^2x_3^2 \\
&+173.205hx_1^2x_2^4 + 200hx_1^3x_2^3 - 173.205hx_2^2x_3^2 \\
&-173.205hx_1^4x_2^2 - 20x_1^2x_2^3x_3 + 20.785x_1^3x_2^2x_3 + 3x_1x_2^4x_3^2 \\
&+1.732x_1^4x_2x_3^2 - 3.464x_1^3x_2^4x_3 + 2x_1^4x_2^3x_3 - 346.41ax_1x_3 \\
&-200ax_2x_3 - 200hx_1x_2 - 3x_1^3x_2^4x_3^2 + 1.732x_1^4x_2^3x_3^2 \\
&+433.013ax_1^2x_2^3x_3^2 - 450ax_1^3x_2^2x_3^2 - 692.82hx_1^2x_2^2x_3^2 \\
&+173.205hx_1^2x_2^4x_3^2 + 200hx_1^3x_2^3x_3^2 - 173.205hx_1^4x_2^2x_3^2 \\
&+519.615ax_1x_2^2x_3 + 500ax_1^2x_2x_3 + 173.205ax_1x_2^4x_3 \\
&+100ax_1^4x_2x_3 - 200hx_1x_2x_3^2 - 450ax_1x_2^2x_3^2 \\
&-433.013ax_1^2x_2x_3^2 - 500ax_1^2x_2^3x_3 + 519.615ax_1^3x_2^2x_3 \\
&+150ax_1x_2^4x_3^2 + 86.602ax_1^4x_2x_3^2 - 346.41ax_1^3x_2^4x_3 \\
&+200ax_1^4x_2^3x_3 + 200hx_1x_2^3x_3^2 - 200hx_1^3x_2x_3^2\Big] \\
&\times t + (1-t) \times G_2 = 0
\end{aligned}$$

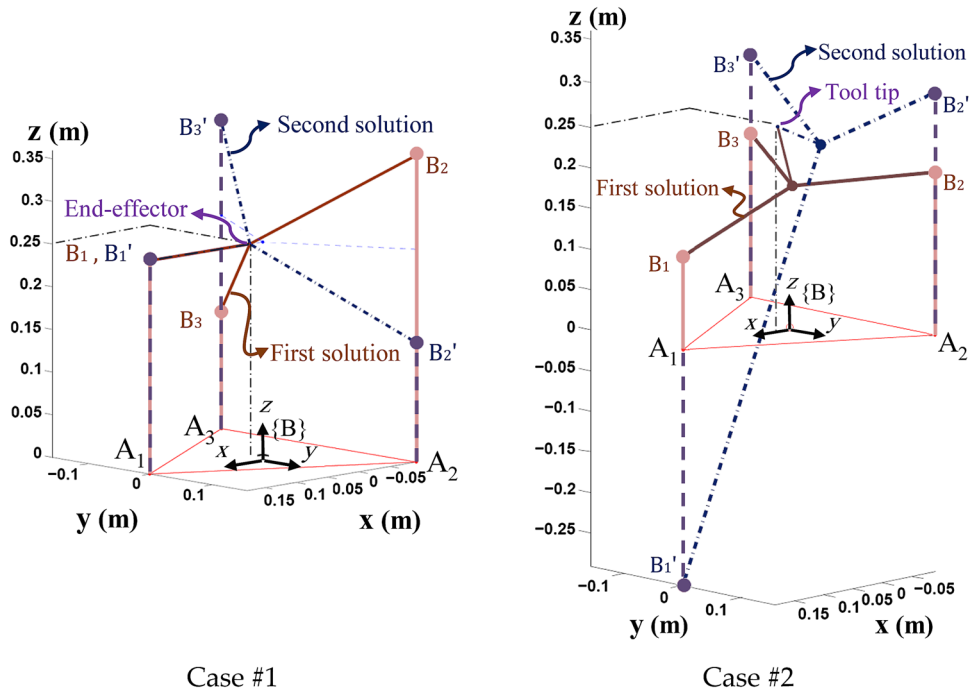

Fig. 7 I-Kin results for mode XYZ

Table 8 The AHFs and their results for operational mode XYZ

	AHFs	Outputs									
	(G_1, G_2, G_3)	(x_1, x_2, x_3)	$\theta°$	$\varphi°$	$\lambda°$	$q_1(m)$	$q_2(m)$	$q_3(m)$	$b_1(m)$	$b_2(m)$	$b_3(m)$
Case#1	(x_1, x_2, x_3)	(0.315, 0, 0)	35.01	0	0	0.25	0.36	0.14	0.161	0.221	0.221
	$(x_1, x_2 - 1, -x_3)$	(−0.315, 0, 0)	**−35.01**	**0**	0	0.25	0.14	0.36	0.161	0.221	0.221
Case#2	(x_1, x_2, x_3)	(0, 0.155, 0)	0	17.65	0	0.115	0.201	0.201	0.194	0.181	0.181
	$(x_1 + 3, -x_2, -x_3)$	(0, 0.641, 0)	0	65.29	0	−0.291	0.299	0.299	0.559	0.181	0.181

I-Kin input values: $x_p = \mathbf{0.02}\,(m)$, $y_p = \mathbf{0}$ and $z_p = \mathbf{0.25}\,(m)$

$$
\begin{aligned}
&\Big[1.732x_2 - 3x_1 - 3x_1^3x_3^2 - 3x_1^3x_2^4 - 1.732x_1^4x_2^3 \\
&\quad -1.732x_2^3x_3^2 - 3.464x_1x_3 + 2x_2x_3 + 150ax_1^3 \\
&\quad +86.602ax_2^3 + 173.205hx_1^2 - 173.205hx_2^2 + 3x_1x_3^2 \\
&\quad +3x_1x_2^4 - 1.732x_2x_3^2 - 3.464x_1^3x_3 - 1.732x_1^4x_2 - 2x_2^3x_3 \\
&\quad +3x_1^3 + 1.732x_2^3 - 450ax_1x_2^2 + 433.013ax_1^2x_2 + 150ax_1x_2^4 \\
&\quad +173.205ax_1^3x_3 - 86.602ax_1^4x_2 + 100ax_2^3x_3 - 200hx_1x_2^3 \\
&\quad +200hx_1^3x_2 + 20.785x_1x_2^2x_3 - 20x_1^2x_2x_3 - 3.464x_1x_2^4x_3 \\
&\quad +2x_1^4x_2x_3 - 433.013ax_1^2x_2^3 - 450ax_1^3x_2^2 - 150ax_1^3x_3^2 \\
&\quad -86.602ax_2^3x_3^2 - 692.82hx_1^2x_2^2 + 173.205hx_1^2x_3^2 \\
&\quad +173.205hx_1^2x_2^4 - 200hx_1^3x_2^3 - 173.205hx_2^2x_3^2 \\
&\quad -173.205hx_1^4x_2^2 + 20x_1^2x_2^3x_3 + 20.785x_1^3x_2^2x_3 - 3x_1x_2^4x_3^2 \\
&\quad +1.732x_1^4x_2x_3^2 - 3.464x_1^3x_2^4x_3 - 2x_1^4x_2^3x_3 - 346.41ax_1x_3 \\
&\quad +200ax_2x_3 + 200hx_1x_2 + 3x_1^3x_2^4x_3^2 + 1.732x_1^4x_2^3x_3^2 \\
&\quad +433.013ax_1^2x_2^3x_3^2 + 450ax_1^3x_2^2x_3^2 - 692.82hx_1^2x_2^2x_3^2 \\
&\quad +173.205hx_1^2x_2^4x_3^2 - 200hx_1^3x_2^3x_3^2 - 173.205hx_1^4x_2^2x_3^2 \\
&\quad +519.615ax_1x_2^2x_3 - 500ax_1^2x_2x_3 + 173.205ax_1x_2^4x_3 \\
&\quad -100ax_1^4x_2x_3 + 200hx_1x_2x_3^2 + 450ax_1x_2^2x_3^2 \\
&\quad -433.013ax_1^2x_2x_3^2 + 500ax_1^2x_2^3x_3 + 519.615ax_1^3x_2^2x_3 \\
&\quad -150ax_1x_2^4x_3^2 + 86.602ax_1^4x_2x_3^2 - 346.41ax_1^3x_2^4x_3 \\
&\quad -200ax_1^4x_2^3x_3 - 200hx_1x_2^3x_3^2 + 200hx_1^3x_2x_3^2\Big] \\
&\quad \times t + (1-t) \times G_3 = 0
\end{aligned}
\tag{38}
$$

Considering I-Kin input values used in Tables 7 and 8 as well as comparing the bold values for the Case#1 in each table, it can be seen that all related variables are equal.

Then, the I-Kin solutions for the case when tool length is nonzero, for the both modes are considered. Results are depicted in Fig. 8 and Table 9. Of course, by looking at Table 9, it can be seen that all related variables for one of the solutions are equal. See bolded numbers.

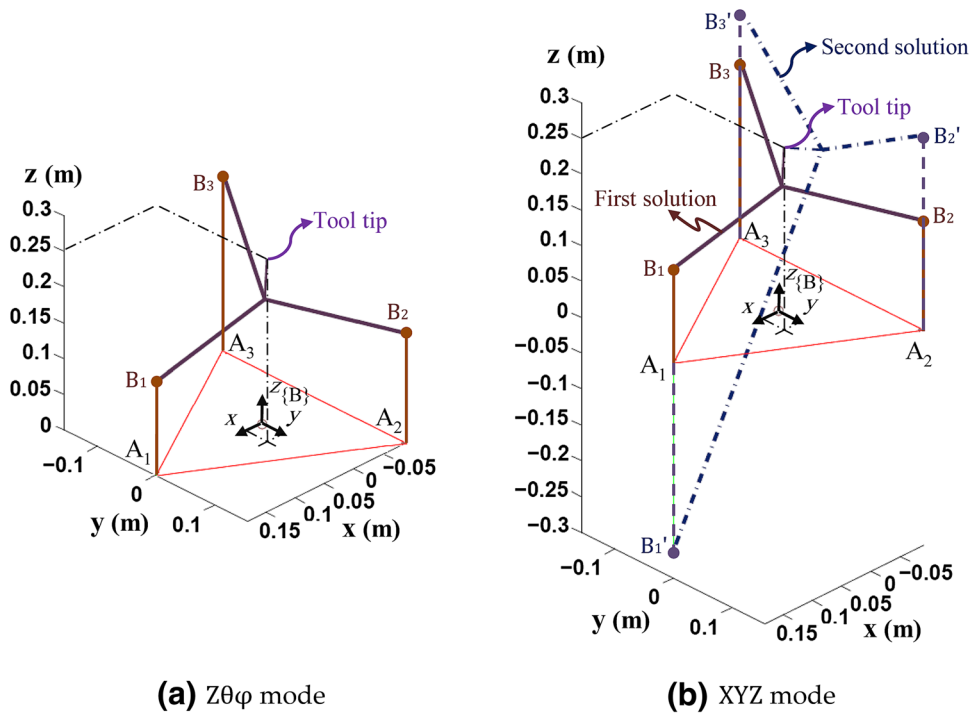

Fig. 8 Comparison between I-Kin answers for modes $\theta\varphi Z$ and XYZ

Table 9 Comparison between I-Kin answers for the $Z\theta\varphi$ and XYZ modes

AHFs	Outputs									
$Z\theta\varphi$ mode										
(G_1, G_2, G_3)	(x_p, y_p, x_3)	$x_P(m)$	$y_P(m)$	$\lambda°$	$q_1(m)$	$q_2(m)$	$q_3(m)$	$b_1(m)$	$b_2(m)$	$b_3(m)$
(x_p, y_p, x_3)	(0.02, 0.03, 0.02)	**0.02**	**0.03**	−2.09	0.132	0.152	0.251	0.185	0.178	0.202
XYZ mode										
(G_1, G_2, G_3)	(x_1, x_2, x_3)	$\theta°$	$\varphi°$	$\lambda°$	$q_1(m)$	$q_2(m)$	$q_3(m)$	$b_1(m)$	$b_2(m)$	$b_3(m)$
$(-x_1, x_2, x_3)$	(−0.15, 0.12, −0.02)	**−17.53**	**13.54**	−2.09	0.132	0.152	0.251	0.185	0.178	0.202
$(-x_1, x_2 - 2, x_3)$	(−0.08, 0.62, −0.05)	−9.5	63.88	−5.93	−0.26	0.27	0.32	0.532	0.15	0.215

I-Kin input values for $Z\theta\varphi$ mode: $\theta° = \mathbf{-17.53}$, $\varphi° = \mathbf{13.54}$ and $z_p = \mathbf{0.25}\,(m)$
I-Kin input values for XYZ mode: $x_p = \mathbf{0.02}\,(m)$, $y_p = \mathbf{0.03}\,(m)$ and $z_p = \mathbf{0.25}\,(m)$
$a = 0.181\,(m)$, $h = 0.08\,(m)$

5 Conclusion

In the present paper, the HCM is applied to both forward and inverse kinematics problems of two different spatial parallel robots. For the F-Kin and the I-Kin, a Stewart platform and the FUM 3-PSP parallel manipulators are studied, respectively. In order to verify results obtained in this paper, the results are compared to that of two published papers. The comparison confirms the findings of this study. The HCM offers few advantages over the conventional methods. It offers a convenient and an effective approach in solving the kinematics problem of spatial parallel robots. The algorithm is quite straightforward and simple while offering a rather high convergence speed. Moreover, it leads to its final values even with poor initial guesses, while the NRM can easily diverge. It was shown for highly nonlinear systems of equations and in the real case situation where we have no good knowledge of the approximate values for the initial guess, the HCM is significantly faster than the NRM. For example, in the F-Kin of the Stewart platform, it is 43% faster than the NRM. It is suggested that to solve the F-Kin of the Stewart platform, for a given joint-space trajectory, it is more computationally efficient to use the combined HCM and the NRM. To do this, the HCM is used to find the answer for the initial point. For the second point, the answer found by HCM for the first point can be used as the initial guess for the NRM method. For all remaining points, the NRM is used where the previous point answer is used as the initial guess for the NRM.

All in all, the proposed method to solve the F-Kin of the Stewart platform leads to a reduction in the F-Kin analysis time required to reach the desired accuracy level. By reducing

the processing time related to solving the F-Kin, more time can be devoted to the control calculations. Therefore, more complicated control algorithms with better performances could be implemented. Results presented in this research confirms that the HCM is a useful method in investigating the kinematics problem of spatial parallel robots. To the best of the authors' knowledge, there does not exist any study for the parallel robots where the proposed hybrid method is used to solve the kinematics problem. As the Stewart robots are perhaps one of the highest used robots in the industry, this solution method potentially can enable additional applications of this robot.

Appendix

Extracting Eq. (34) and substituting rotation matrix components, constraint equations, which are nine nonlinear algebraic equations, can be obtained as follows,

$$\boldsymbol{\psi}\,(\mathbf{q}) = \mathbf{0} \tag{39}$$

where

$$\begin{aligned}
\psi_1 &= x_{\mathrm{P}} + b_1\,(\cos(\varphi)\cos(\lambda)) - h\,(\sin(\theta)\sin(\lambda) \\
&\quad + \sin(\varphi)\cos(\theta)\cos(\lambda)) - a = 0 \\
\psi_2 &= y_{\mathrm{P}} + b_1\,(\cos(\varphi)\sin(\lambda)) - h\,(-\sin(\theta)\cos(\lambda) \\
&\quad + \sin(\varphi)\cos(\theta)\sin(\lambda)) = 0 \\
\psi_3 &= z_{\mathrm{P}} + b_1\,(-\sin(\varphi)) - h\,(\cos(\varphi)\cos(\theta)) - q_1 = 0 \\
\psi_4 &= x_{\mathrm{P}} - \frac{1}{2}\,b_2\,(\cos(\varphi)\cos(\lambda)) + \frac{\sqrt{3}}{2}\,b_2\,(-\cos(\theta)\sin(\lambda) \\
&\quad + \sin(\varphi)\sin(\theta)\cos(\lambda)) - h\,(\sin(\theta)\sin(\lambda) \\
&\quad + \sin(\varphi)\cos(\theta)\cos(\lambda)) + \frac{1}{2}\,a = 0 \\
\psi_5 &= y_{\mathrm{P}} - \frac{1}{2}\,b_2\,(\cos(\varphi)\sin(\lambda)) + \frac{\sqrt{3}}{2}\,b_2\,(\cos(\theta)\cos(\lambda) \\
&\quad + \sin(\varphi)\sin(\theta)\sin(\lambda)) - h\,(-\sin(\theta)\cos(\lambda) \\
&\quad + \sin(\varphi)\cos(\theta)\sin(\lambda)) - \frac{\sqrt{3}}{2}\,a = 0 \\
\psi_6 &= z_{\mathrm{P}} - \frac{1}{2}\,b_2\,(-\sin(\varphi)) + \frac{\sqrt{3}}{2}\,b_2\,(\cos(\varphi)\sin(\theta)) \\
&\quad - h\,(\cos(\varphi)\cos(\theta)) - q_2 = 0 \\
\psi_7 &= x_{\mathrm{P}} - \frac{1}{2}\,b_3\,(\cos(\varphi)\cos(\lambda)) - \frac{\sqrt{3}}{2}\,b_3\,(-\cos(\theta)\sin(\lambda) \\
&\quad + \sin(\varphi)\sin(\theta)\cos(\lambda)) - h\,(\sin(\theta)\sin(\lambda) \\
&\quad + \sin(\varphi)\cos(\theta)\cos(\lambda)) + \frac{1}{2}\,a = 0 \\
\psi_8 &= y_{\mathrm{P}} - \frac{1}{2}\,b_3\,(\cos(\varphi)\sin(\lambda)) - \frac{\sqrt{3}}{2}\,b_3\,(\cos(\theta)\cos(\lambda) \\
&\quad + \sin(\varphi)\sin(\theta)\sin(\lambda)) - h\,(-\sin(\theta)\cos(\lambda) \\
&\quad + \sin(\varphi)\cos(\theta)\sin(\lambda)) + \frac{\sqrt{3}}{2}\,a = 0 \\
\psi_9 &= z_{\mathrm{P}} - \frac{1}{2}\,b_3\,(-\sin(\varphi)) - \frac{\sqrt{3}}{2}\,b_3\,(\cos(\varphi)\sin(\theta)) \\
&\quad - h\,(\cos(\varphi)\cos(\theta)) - q_3 = 0
\end{aligned} \tag{40}$$

$$\begin{aligned}
&x_3 - 50ax_3 - 50hx_1 + x_1^2x_3 - 50ax_1^2x_3 - 50hx_1x_2^2 = 0 \\
&3x_1 + 1.732x_2 + 3x_1^3x_3^2 + 3x_1^3x_2^4 - 1.732x_1^4x_2^3 - 1.732x_2^3x_3^2 \\
&\quad - 3.464x_1x_3 - 2x_2x_3 - 150ax_1^3 + 86.602ax_2^3 + 173.205hx_1^2 \\
&\quad - 173.205hx_2^2 - 3x_1x_3^2 - 3x_1x_2^4 - 1.732x_2x_3^2 - 3.464x_1^3x_3 \\
&\quad - 1.732x_1^4x_2 + 2x_2^3x_3 - 3x_1^3 + 1.732x_2^3 + 450ax_1x_2^2 \\
&\quad +433.013ax_1^2x_2 - 150ax_1x_2^4 + 173.205ax_1^3x_3 - 86.602ax_1^4x_2 \\
&\quad - 100ax_2^3x_3 + 200hx_1x_2^3 - 200hx_1^3x_2 + 20.785x_1x_2^2x_3 \\
&\quad + 20x_1^2x_2x_3 - 3.464x_1x_2^4x_3 - 2x_1^4x_2x_3 - 433.013ax_1^2x_2^3 \\
&\quad + 450ax_1^3x_2^2 + 150ax_1^3x_3^2 - 86.602ax_2^3x_3^2 \\
&\quad - 692.82hx_1^2x_2^2 + 173.205hx_1^2x_3^2 + 173.205hx_1^2x_2^4 + 200hx_1^3x_2^3 \\
&\quad - 173.205hx_2^2x_3^2 - 173.205hx_1^4x_2^2 - 20x_1^2x_2^3x_3 + 20.785x_1^3x_2^2x_3 \\
&\quad + 3x_1x_2^4x_3^2 + 1.732x_1^4x_2x_3^2 - 3.464x_1^3x_2^4x_3 + 2x_1^4x_2^3x_3 \\
&\quad - 346.41ax_1x_3 - 200ax_2x_3 - 200hx_1x_2 - 3x_1^3x_2^4x_3^2 \\
&\quad + 1.732x_1^4x_2^3x_3^2 + 433.013ax_1^2x_2^3x_3^2 - 450ax_1^3x_2^2x_3^2 \\
&\quad - 692.82hx_1^2x_2^2x_3^2 + 173.205hx_1^2x_2^4x_3^2 + 200hx_1^3x_2^3x_3^2 \\
&\quad - 173.205hx_1^4x_2^2x_3^2 + 519.615ax_1x_2^2x_3 + 500ax_1^2x_2x_3 \\
&\quad + 173.205ax_1x_2^4x_3 + 100ax_1^4x_2x_3 - 200hx_1x_2x_3^2 \\
&\quad - 450ax_1x_2^2x_3^2 - 433.013ax_1^2x_2x_3^2 - 500ax_1^2x_2^3x_3 \\
&\quad + 519.615ax_1^3x_2^2x_3 + 150ax_1x_2^4x_3^2 + 86.602ax_1^4x_2x_3^2 \\
&\quad - 346.41ax_1^3x_2^4x_3 + 200ax_1^4x_2^3x_3 + 200hx_1x_2^3x_3^2 \\
&\quad - 200hx_1^3x_2x_3^2 = 0 \\
&1.732x_2 - 3x_1 - 3x_1^3x_3^2 - 3x_1^3x_2^4 - 1.732x_1^4x_2^3 - 1.732x_2^3x_3^2 \\
&\quad - 3.464x_1x_3 + 2x_2x_3 + 150ax_1^3 + 86.602ax_2^3 + 173.205hx_1^2 \\
&\quad - 173.205hx_2^2 + 3x_1x_3^2 + 3x_1x_2^4 - 1.732x_2x_3^2 - 3.464x_1^3x_3 \\
&\quad - 1.732x_1^4x_2 - 2x_2^3x_3 + 3x_1^3 + 1.732x_2^3 - 450ax_1x_2^2 \\
&\quad + 433.013ax_1^2x_2 + 150ax_1x_2^4 + 173.205ax_1^3x_3 - 86.602ax_1^4x_2 \\
&\quad + 100ax_2^3x_3 - 200hx_1x_2^3 + 200hx_1^3x_2 + 20.785x_1x_2^2x_3 \\
&\quad - 20x_1^2x_2x_3 - 3.464x_1x_2^4x_3 + 2x_1^4x_2x_3 - 433.013ax_1^2x_2^3 \\
&\quad - 450ax_1^3x_2^2 - 150ax_1^3x_3^2 - 86.602ax_2^3x_3^2 - 692.82hx_1^2x_2^2 \\
&\quad + 173.205hx_1^2x_3^2 + 173.205hx_1^2x_2^4 - 200hx_1^3x_2^3 \\
&\quad - 173.205hx_2^2x_3^2 - 173.205hx_1^4x_2^2 + 20x_1^2x_2^3x_3 + 20.785x_1^3x_2^2x_3 \\
&\quad - 3x_1x_2^4x_3^2 + 1.732x_1^4x_2x_3^2 - 3.464x_1^3x_2^4x_3 - 2x_1^4x_2^3x_3 \\
&\quad - 346.41ax_1x_3 + 200ax_2x_3 + 200hx_1x_2 + 3x_1^3x_2^4x_3^2 \\
&\quad + 1.732x_1^4x_2^3x_3^2 + 433.013ax_1^2x_2^3x_3^2 + 450ax_1^3x_2^2x_3^2 \\
&\quad - 692.82hx_1^2x_2^2x_3^2 + 173.205hx_1^2x_2^4x_3^2 - 200hx_1^3x_2^3x_3^2 \\
&\quad - 173.205hx_1^4x_2^2x_3^2 + 519.615ax_1x_2^2x_3 - 500ax_1^2x_2x_3 \\
&\quad + v173.205ax_1x_2^4x_3 - 100ax_1^4x_2x_3 + 200hx_1x_2x_3^2 + 450ax_1x_2^2x_3^2 \\
&\quad - 433.013ax_1^2x_2x_3^2 + 500ax_1^2x_2^3x_3 + 519.615ax_1^3x_2^2x_3
\end{aligned}$$

$$-150ax_1x_2^4x_3^2 + 86.602ax_1^4x_2x_3^2 - 346.41ax_1^3x_2^4x_3 - 200ax_1^4x_2^3x_3 - 200hx_1x_2^3x_3^2 + 200hx_1^3x_2x_3^2 = 0 \quad (41)$$

References

1. Rezaei A, Akbarzadeh A, Akbarzadeh-T M-R (2012) An investigation on stiffness of a 3-PSP spatial parallel mechanism with flexible moving platform using invariant form. Mech Mach Theory 51:195–216
2. Stewart D (1965) A platform with six degrees of freedom. Proc Inst Mech Eng 180(1):371–386
3. Nanua P, Waldron KJ, Murthy V (1990) Direct kinematic solution of a Stewart platform. IEEE Trans Robot Autom 6(4):438–444
4. Zhang C, Song S (1992) Forward kinematics of a class of parallel (Stewart) platforms with closed-form solutions. J Robot Syst 9(1):93–112
5. Liu K, Fitzgerald JM, Lewis FL (1993) Kinematic analysis of a Stewart platform manipulator. IEEE Trans Ind Electron 40(2):282–293
6. Raghavan M (1993) The Stewart platform of general geometry has 40 configurations. J Mech Des 115(2):277–282
7. Wampler CW (1996) Forward displacement analysis of general six-in-parallel SPS (Stewart) platform manipulators using soma coordinates. Mech Mach Theory 31(3):331–337
8. Husty ML (1996) An algorithm for solving the direct kinematics of general Stewart-Gough platforms. Mech Mach Theory 31(4):365–379
9. Yee CS, Lim K-B (1997) Forward kinematics solution of Stewart platform using neural networks. Neurocomputing 16(4):333–349
10. Dhingra AK, Almadi AN, Kohli D (2000) A Grobner–Sylvester hybrid method for closed-form displacement analysis of mechanisms. J Mech Des 122(4):431–438
11. Ji P, Wu H (2001) A closed-form forward kinematics solution for the 6–6 Stewart platform. IEEE Trans Robot Autom 17(4):522–526
12. Innocenti C (2001) Forward kinematics in polynomial form of the general Stewart platform. J Mech Des 123(2):254–260
13. Lee T-Y, Shim J-K (2001) Forward kinematics of the general 6–6 Stewart platform using algebraic elimination. Mech Mach Theory 36(9):1073–1085
14. Gao X-S, Lei D, Liao Q, Zhang G-F (2005) Generalized Stewart-Gough platforms and their direct kinematics. IEEE Trans Robot 21(2):141–151
15. Wang Y (2007) A direct numerical solution to forward kinematics of general Stewart-Gough platforms. Robotica 25(1):121–128
16. Omran A, Bayoumi M, Kassem A, El-Bayoumi G (2009) Optimal forward kinematics modeling of Stewart manipulator using genetic algorithms. Jordan J Mech Ind Eng 3(4):280–293
17. Huang X, Liao Q, Wei S (2010) Closed-form forward kinematics for a symmetrical 6–6 Stewart platform using algebraic elimination. Mech Mach Theory 45(2):327–334
18. Zhang YH, Guan LW, Wang LP, Hua YZ (2013) Research on the forward kinematics of Stewart platform using memetic algorithms. Appl Mech Mater 268:1416–1421
19. Zhou W, Chen W, Liu H, Li X (2015) A new forward kinematic algorithm for a general Stewart platform. Mech Mach Theory 87:177–190
20. Kardan I, Akbarzadeh A (2015) An improved hybrid method for forward kinematics analysis of parallel robots. Adv Robot 29(6):401–411
21. Rezaei A, Akbarzadeh A, Nia PM, Akbarzadeh MRT (2013) Position, Jacobian and workspace analysis of a 3-PSP spatial parallel manipulator. Robot Comput Integr Manuf 29(4):158–173
22. Rezaei A, Akbarzadeh A (2015) Study on Jacobian, singularity and kinematics sensitivity of the FUM 3-PSP parallel manipulator. Mech Mach Theory 86:211–234
23. Toutounian F, Saberi-Nadjafi J, Taheri SH (2009) A hybrid of the Newton-GMRES and electromagnetic meta-heurestic methods for solving systems of nonlinear equations. J Math Model Algorithms 8(4):425–443
24. Bonev IA (2002) Geometric analysis of parallel mechanims. PhD thesis, Laval University
25. Gregorio RD, Parenti-Castelli V (2001) Position analysis in analytical form of the 3-PSP mechanism. J Mech Des 123(1):51–57
26. Bin D, Xiang-de Z (2001) Continuation method applied in kinematics of parallel robot. Appl Math Mech 22(12):1422–1428
27. Abbasnejad G, Zarkandi S, Imani M (2010) Forward kinematics analysis of a 3-PRS parallel manipulator. World Acad Sci Eng Technol 37:329–335
28. Varedi S, Daniali H, Ganji D (2009) Kinematics of an offset 3-UPU translational parallel manipulator by the homotopy continuation method. Nonlinear Anal Real World Appl 10(3):1767–1774
29. Wu T-M (2006) The inverse kinematics problem of spatial 4P3R robot manipulator by the homotopy continuation method with an adjustable auxiliary homotopy function. Nonlinear Anal 64(10):2373–2380
30. Wu T-M (2006) Solving the nonlinear equations by the Newton-homotopy continuation method with adjustable auxiliary homotopy function. Appl Math Comput 173(1):383–388
31. Wu T-M (2005) A study of convergence on the Newton-homotopy continuation method. Appl Math Comput 168(2):1169–1174